Tenth MSU Conference on Differential Equations and Computational Simulations.
Electronic Journal of Differential Equations, Conference 23 (2016), pp. 119–129.
ISSN: 1072-6691. URL: http://ejde.math.txstate.edu or http://ejde.math.unt.edu
ftp ejde.math.txstate.edu

FAST SOLUTION OF PHASE UNWRAPPING PARTIAL DIFFERENTIAL EQUATION USING WAVELETS

MARYAM RAHNEMOONFAR

Abstract. Phase unwrapping is the most critical step in the processing of synthetic aperture radar interferometry. The phase obtained by SAR interferometry is wrapped over a range from $-\pi$ to π. Phase unwrapping must be performed to obtain the true phase. The least square approach attains the unwrapped phase by minimizing the difference between the discrete partial derivatives of the wrapped phase and the discrete partial derivatives of the unwrapped solution. The least square solution will result in discrete version of the Poisson's partial differential equation. Solving the discretized Poisson's equation with the classical method of Gauss-Seidel relaxation has extremely slow convergence. In this paper we have used Wavelet techniques which overcome this limitation by transforming low-frequency components of error into high frequency components which consequently can be removed quickly by using the Gauss-Seidel relaxation method. In Discrete Wavelet Transform (DWT) two operators, decomposition (analysis) and reconstruction (synthesis), are used. In the decomposition stage an image is separated into one low-frequency component (approximation) and three high-frequency components (details). In the reconstruction stage, the image is reconstructed by synthesizing the approximated and detail components. We tested our algorithm on both simulated and real data and on both unweighted and weighted forms of discretized Poisson's equation. The experimental results show the effectiveness of the proposed method.

1. Introduction

Due to the nature of SAR imaging, it does not contain information about the absolute phase of the returning radar echoes, but the phase is wrapped to the interval $[-\pi, \pi]$. Reconstruction of the absolute phase from the wrapped phase value is called phase unwrapping. Phase unwrapping is the key step in interferometric synthetic aperture radar (InSAR) processing. InSAR is a technique that uses two or more SAR images over the same area for extracting high-resolution digital terrain data. The technique relies on the measurement of the phase of the echoed signal rather than its amplitude, as found in conventional imaging radar system. The extreme sensitivity of the technique to altitude changes, high spatial resolution and broad swath coverage makes it an extensive and accurate measurement

2010 *Mathematics Subject Classification.* 65T60, 35-04.
Key words and phrases. Wavelets.

Published March 21, 2016.

means in many fields; namely earthquake monitoring, erosion studies, and mining prospecting. The technique brings strong advantages such as independency of natural illumination or recognizable targets over classical stereoscopic optical imaging.

A variety of approaches to 2-D phase unwrapping have been proposed recently. They can be classified to path-following and least-squares methods, respectively. Path-following algorithms [1, 5, 6] are based on the identification of residues, local errors in the measured phase caused by signal noise or by actual discontinuities, and the definition of suitable branch cuts to prevent any integration path crossing these cuts. The estimated neighboring pixel differences of unwrapped phase are integrated along paths avoiding the branch cuts where these estimated differences are inconsistent [5]. The problems of this approach are the definition of suitable branch cuts and the time consuming computations.

The least-squares method is based on partial differential equation which extracts the phase partial derivatives and then finds the unwrapped surface that best fits these derivatives. This technique was introduced in the late 70's by Fried and Hudgin [2, 7] and later refined in 1989 and 1994 by Ghiglia and Romero [3, 4]. Because this approach does not depend on path-following or branch-cutting techniques, it is reliable. To accelerate the convergence of solution of the phase unwrapping partial differential equation, direct methods based on the fast Fourier transform (FFT) [11] or the discrete cosine transform (DCT) [4] can be applied. Despite its robustness and speed, the technique has an inadequacy of unwrapping through phase inconsistencies rather than unwrapping around them that causes errors in the unwrapped surface. This problem is overcome by introducing weight functions. In the weighted case, direct methods cannot be used and iterative methods should be adopted. Gauss-Seidel relaxation is the classical iterative method for solving the linear system. Due to its extremely slow convergence, Gauss-Seidel relaxation is not a practical method but it can be base of some practical algorithms such as multigrid [10] or wavelet [8, 12] for solving the weighted least squares phase unwrapping. The multigrid method is an efficient algorithm to improve convergence rate. However, this method needs an additional weight restriction operator which is very complicated and can be erroneous.

In this article, wavelet technique is used for the fast solution of phase unwrapping partial differential equation. Wavelet technique overcomes the limitation of slow convergence of Gauss-Seidel relaxation by transforming low-frequency components of error into high frequency components which consequently will be removed quickly by using the Gauss-Seidel relaxation method. In Discrete Wavelet Transform (DWT) two operators, decomposition (analysis) and reconstruction (synthesis), are used. In the decomposition stage an image is separated into one low-frequency component (approximation) and three high-frequency components (details). In the reconstruction stage, the image is reconstructed by synthesizing the approximated and detail components. In this paper the proposed phase unwrapping approach is applied both on simulated and real data. Moreover, a post-processing step is applied to the wavelet unwrapped phase to ensure the congruency of the unwrapped phase to the wrapped phase. Another correction model is also introduced to remove the error - caused by atmosphere, phase and baseline - and to improve the accuracy of the generated DEM. After this short introduction, phase

unwrapping concept and the proposed wavelet technique for both weighted and unweighted least square are explained in section 2. Experimental results are presented in section 3, Finally conclusion is drawn.

2. Phase unwrapping

The first step of a typical InSAR processing routine is the co-registration of the slave image over the master one and computation of the interferogram by multiplying the complex value of the master image by the complex conjugate number of the corresponding pixel in the slave image. This Interferogram should undergo a flat earth correction, which is the removal of strong contribution due to the slant range geometry using the orbit data. An interferogram contains phase information which is directly related to topography. Since this phase is given in modulo 2π, there is an ambiguity in calculating the correct integer number of 2π phase cycles that need to be added to each phase measurement in order to obtain the correct slant range distance. This ambiguity solution is referred to as phase unwrapping which is an important issue in the derivation of elevations using the InSAR technique.

The problem of phase unwrapping has been the focus of InSAR research for several years. Numerous methods were proposed and implemented for the most complex issue of the interferometric processing chain. The two major approaches are "path-following" and "least-squares" algorithms. Path-following algorithms use localized pixel-by-pixel operations to unwrap the phase, while least-squares algorithms minimize a global measure of the differences between the gradients of the wrapped input phase and those of the unwrapped solution. In this article, we use a wavelet algorithm for solving the two dimensional least-squares phase unwrapping.

Let us assume that the phase of interferogram, $\psi_{i,j}$, which is between $-\pi$ and π is known. We want to determine the unwrapped phase value, $\varphi_{i,j}$, at the same grid locations

$$\psi_{i,j} = \varphi_{i,j} + 2\pi k, \tag{2.1}$$

where k is an integer and $-\pi < \psi_{i,j} < \pi$. The least square approach attains this unwrapped phase by minimizing the difference between the discrete partial derivatives of the wrapped phase and the discrete partial derivatives of the unwrapped solution. The partial derivatives of the wrapped phase is

$$\Delta x_{i,j} = \psi_{i+1,j} - \psi_{i,j}\ , \quad \Delta y_{i,j} = \psi_{i,j+1} - \psi_{i,j} \tag{2.2}$$

The differences are defined at the boundaries by means of boundary conditions:

$$\begin{aligned} \Delta^x_{0j} = -\Delta^x_{1j}, \quad \Delta^y_{i0} = -\Delta^y_{i1}, \\ \Delta^x_{M=1,j} = -\Delta^x_{Mj}, \quad \Delta^y_{i,N+1} = -\Delta^y_{iN}. \end{aligned} \tag{2.3}$$

The difference between these partial derivatives and the partial derivatives of the solution must be minimized in the least square sense:

$$\sum_i \sum_j (\varphi_{i,j} - \varphi_{i-1,j} - \Delta x_{i,j})^2 + \sum_i \sum_j (\varphi_{i,j} - \varphi_{i,j-1} - \Delta y_{i,j})^2 \tag{2.4}$$

Differentiating the above sum with respect to $\varphi_{i,j}$ and setting the result equal to zero, the following equation is obtained:

$$(\varphi_{i+1,j} - 2\varphi_{i,j} + \varphi_{i-1,j}) + (\varphi_{i,j+1} - 2\varphi_{i,j} + \varphi_{i,j-1}) = \rho_{i,j} \tag{2.5}$$

where $\rho_{i,j}$ is equal to:

$$\rho_{i,j} = (\Delta x_{i+1,j} - \Delta x_{i,j} + \Delta y_{i,j+1} - \Delta y_{i,j}) \tag{2.6}$$

The values of the solution array at the boundaries are defined by the boundary conditions

$$\begin{aligned} \varphi_{-1,j} = \varphi_{1,j}, \quad \varphi_{i,-1} = \varphi_{i,1}, \\ \varphi_{M+1,j} = \varphi_{M-1,j}, \quad \varphi_{i,N+1} = \varphi_{i,N-1}. \end{aligned} \tag{2.7}$$

Equation (2.5) is a discretization of the Poisson equation in a rectangular grid:

$$\frac{\partial^2}{\partial x^2}\varphi(x,y) + \frac{\partial^2}{\partial y^2}\varphi(x,y) = \rho(x,y) \tag{2.8}$$

Writing the above equation in matrix format yields the equation

$$A\varphi = \rho \tag{2.9}$$

where A is a sparse matrix and φ is the solution of phase unwrapping. The classical method for solving the discretized Poisson equation is Gauss-Seidel relaxation. Due to its extremely slow convergence, Gauss-Seidel relaxation is not a practical method, but it is the base of the wavelet method. The Gauss-Seidel relaxation is essentially a local smoothing operator that removes the high-frequency components of the error very rapidly but the low-frequency components extremely slowly. The wavelet technique overcomes this limitation by transforming low-frequency components of error into high-frequency components which consequently can be removed quickly by using the Gauss-Seidel relaxation method.

2.1. **Wavelet phase unwrapping.** The wavelet theory allows a very general and flexible description to transform signals from a time domain to a time-frequency domain, so-called time-scale domain. The representation is a suitable alternative to the window Fourier transform. Wavelet transform uses short window for high frequencies, leading to a good time resolution and larger windows for low frequencies leading to a good frequency resolution. The one-dimensional continuous wavelet transform of a signal $x(t)$ is defined by [9]

$$\begin{aligned} W_\psi(a,b) &= \int_{-\infty}^{+\infty} x(t)\psi^*_{a,b}(t)dt \\ \psi_{a,b}(t) &= \frac{1}{\sqrt{|a|}}\psi(\frac{t-b}{a}) \end{aligned} \tag{2.10}$$

where $\psi_{a,b}(t)$ stands for a given wavelet function and a and b are the scale and translation parameters, respectively. The wavelet transform provides the time-frequency information of a signal simultaneously. The continuous wavelet transform is computed by changing the scale of analysis window, shifting the window in time, multiplying by the signal and integrating over all the times. It is essentially a measure of correlation between a signal and various wavelets derived from a mother. In Discrete Wavelet Transform (DWT), this is turned into a filtering operation with a sequence of high-pass and low-pass filters of different cut-off frequencies to analyze the signal at different scales. The signal is passed through a series of high pass filters and low pass filters. Filtering a signal corresponds to the convolution of the signal with impulse response of a filter. The DWT is computed as the signals at different frequency bands with different resolutions by decomposing them into approximation and detail components. The decomposition is achieved at successive

high pass and low pass filtering of the time domain signal. The approximation and detail components are convolved recursively with the same low-pass and high-pass filters until they reach a certain level. The discrete form of equation (2.10) can be written as:

$$\begin{aligned} ca_{j,k}[x(t)] &= DS[\sum x(t)\ g_j^*(t-2^j k)] \\ cd_{j,k}[x(t)] &= DS[\sum x(t)\ h_j^*(t-2^j k)] \end{aligned} \tag{2.11}$$

where the coefficients $ca_{j,k}$ and $cd_{j,k}$ specify approximation and details components provided by the $g(n)$ low-pass and $h(n)$ high-pass impulse responses, respectively, and the DS operator performs downsampling by a factor of 2. The one-dimensional wavelet decomposition is extended to an image by applying it first to the row-direction and next to the column-direction. For the decomposition in stage one, we first convolve the rows of the image with low-pass and high-pass filters and discard the odd-numbered columns (downsample) of the two resulting arrays (Figure 1). The columns of each of the $N/2$-by-N arrays are then convolved with low-pass and high-pass filters and the odd numbered rows are discarded. The result is the four $N/2$-by-$N/2$ subimages which are approximation-approximation (LL), approximation-detail (LH), detail-approximation (HL), and detail-detail (HH) components. The one level decomposition of an image is depicted in Figure 1.

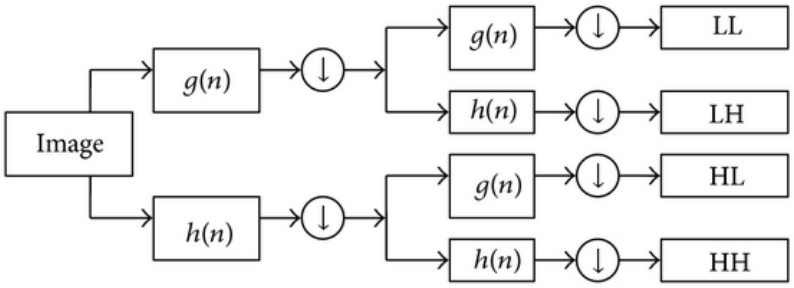

FIGURE 1. Two dimensional discrete wavelet decomposition.

The obtained approximation images can be decomposed again to obtain second-level detail and approximation images, and the process can be repeated for finer analysis as each iteration double the image scale.

In the reconstruction stage, the image is reconstructed by synthesizing the approximated and detail components. The transformed coefficients are recovered to the original signal under the reconstruction procedure. At each level, the approximation component is convolved with the low-pass filter and the detail component is convolved with the high-pass filter. After the filtering, each part is oversampled by a factor of two and added to generate the approximation signal of the next higher level.

Gauss-Seidel relaxation is a local smoothing operator that removes the high-frequency components of the error very rapidly but the low-frequency components extremely slowly. Wavelet techniques overcome this limitation by transforming low-frequency components of error into high-frequency components which consequently

can be removed quickly by using the Gauss-Seidel relaxation method. For solving equation (2.9) by wavelet algorithm, after relaxing v_1 times on the equation (2.9) with the initial guess 0, the residual error of this equation is transformed by the decomposition step of the DWT into the second level. Then, further relaxation is performed on the residual equation $Ae = r$ in the low-frequency component (LL) of the second level with the initial guess $e = 0$, where $r = \rho - A\hat{\varphi}$ is the known residual error. The resulting solution of the lower component of the coarser grid is regarded as an intermediate solution whose residual error is transformed to the third level with DWT. This process continues until we reach the coarsest grid. At this point the solution is then transferred to the finer grid by the reconstruction analysis of DWT; ultimately, it will be added to the approximation $\hat{\varphi}$. This process yields a better solution on the finer grid.

2.2. **Weighted wavelet phase unwrapping.** The weighted least square approach attains the unwrapped phase by minimizing the difference between the discrete partial derivatives of the wrapped phase and the discrete partial derivatives of the unwrapped solution. The solution $\varphi_{i,j}$ that minimizes $\mathcal{L}$ is the weighted least square solution, where $\mathcal{L}$ is

$$\begin{aligned}\mathcal{L} = &\sum_i \sum_j w^x_{i,j}(\varphi_{i,j} - \varphi_{i-1,j} - \Delta x_{i,j})^2 \\ &+ \sum_i \sum_j w^y_{i,j}(\varphi_{i,j} - \varphi_{i,j-1} - \Delta y_{i,j})^2\end{aligned} \tag{2.12}$$

where w^x and w^y are weight functions and Δx and Δy are the partial derivatives of the wrapped phase:

$$\begin{aligned}\Delta x_{i,j} &= W\{\psi_{i+1,j} - \psi_{i,j}\} \\ \Delta y_{i,j} &= W\{\psi_{i,j+1} - \psi_{i,j}\}\end{aligned} \tag{2.13}$$

where W is the wrapping operator. The least squares solution of (2.12) yields the equation

$$\begin{aligned}&w^x_{i,j}(\varphi_{i+1,j} - \varphi_{i,j}) - w^x_{i-1,j}(\varphi_{i,j} - \varphi_{i-1,j}) \\ &+ w^y_{i,j}(\varphi_{i,j+1} - \varphi_{i,j}) - w^x_{i,j-1}(\varphi_{i,j} - \varphi_{i,j-1}) = \rho_{i,j}\end{aligned} \tag{2.14}$$

where

$$\rho_{i,j} = w^x_{i,j}\Delta x_{i,j} - w^x_{i-1,j}\Delta x_{i-1,j} + w^y_{i,j}\Delta y_{i,j} - w^y_{i,j-1}\Delta y_{i,j-1} \tag{2.15}$$

Equation (2.14) is a weighted and discrete version of the Poisson's partial differential equation (PDE) which in matrix format yields the equation

$$B\varphi = \rho \tag{2.16}$$

where B is a sparse matrix and φ is the solution of phase unwrapping.

As it can be seen from equation(2.16), the weight array is embedded in the matrix B, and the wavelet decomposition of B conducts the decomposition of the weight array simultaneously. Therefore, the reduction of the weight array to a smaller scale is accomplished automatically and the separate weight reduction operation is not required. Therefore solving this equation with wavelet transform is similar to unweighted case. Because the least-squares solution minimizes the squares of the differences between the gradients of the solution and the phase, the solutions are not congruent to the wrapped phase [10]. Therefore, after solving equation (2.16) with a wavelet algorithm, it is necessary to perform a post-processing step

by subtracting the solution from the wrapped input phase, rewrapping the result, and then adding it back into the solution.

3. Experimental results

In this section we present the results of wavelet algorithm on several dataset including simulated data, SAR interferometry and differential SAR interferometry.

3.1. **Simulated Data.** In the first example, the phase pattern of pixels is simulated as shown in figure 2(a). Then the phase was wrapped to the interval of $-\pi$ to π (figure 2(b)). To evaluate the performance of the proposed method, we unwrapped the phase using wavelet technique and then compared it with the Gauss-Seidel, and multigrid[10] methods. The reconstructed phase pattern via Gauss-Seidel, multigrid and wavelet method with the same number of iterations (100 iterations) are shown in 2(a). Comparing the results with the original shape (figure 2(a)), we achieved the average of 2.88 and 2.10 differences (error) for multigrid and wavelet methods, respectively. This shows that the wavelet method is more accurate than the multigrid and it converges faster.

In other experiment a terrain model is generated with fractal (figure 3(a)). The phase is wrapped to the interval of $-\pi$ to π to simulate the interferogram (Figure 3(b)). In this case a weighted wavelet and multigrid method is used. Figures 3(c) and 3(d) show the weights in x and y direction. Weights are extracted by variance of phase derivatives in x any y direction. Figure 3(e) shows the reconstructed phase pattern of wavelet method. In this case the RMS error for wavelets is 0.62 while it is 0.66 for multigrid that shows a better solution of wavelet in weighted case. It is explained in previous section that the least squares solutions are not congruent to the wrapped input phase, so a post-processing step was done on two results. The RMS errors after the post-processing step are 0.13 and 0.24 for wavelet and multigrid, respectively.

3.2. **Real data.** In the second part of the experimental results, the proposed method was tested on some real data. In the first part, two single look complex SAR images of ENVISAT ASAR data are used to generate Digital Elevation Model (DEM). In the second part three single look complex SAR images of ENVISAT ASAR data are used to create differential interferogram to study earthquake.

3.3. **Digital elevation model.** SAR Interferometry is based on the measurement of phase differences caused by a path difference, in the slant range direction, of the radar signal. A path difference, and consequently an interferometric pattern, can be caused by a slight change in the angle under which the same terrain is seen in the two images (Figure 4). By considering images taken from the sensor at two slightly different positions we can deduce the height of the terrain. This approach of InSAR is used to produce Digital Elevation Models (or DEM's) of the surface. The phase fringes, obtained in this way after phase unwarpping stage, are directly related to the terrain height.

In this experiment, two single look complex SAR images of ENVISAT ASAR data were used for creating DEM. After co-registration of two images and creating interferogram, the filtered interferograms were unwrapped using the weighted wavelet algorithm. The coherence map of the area is used for weight function. Coherence map is created based on the correlation between two images. For both

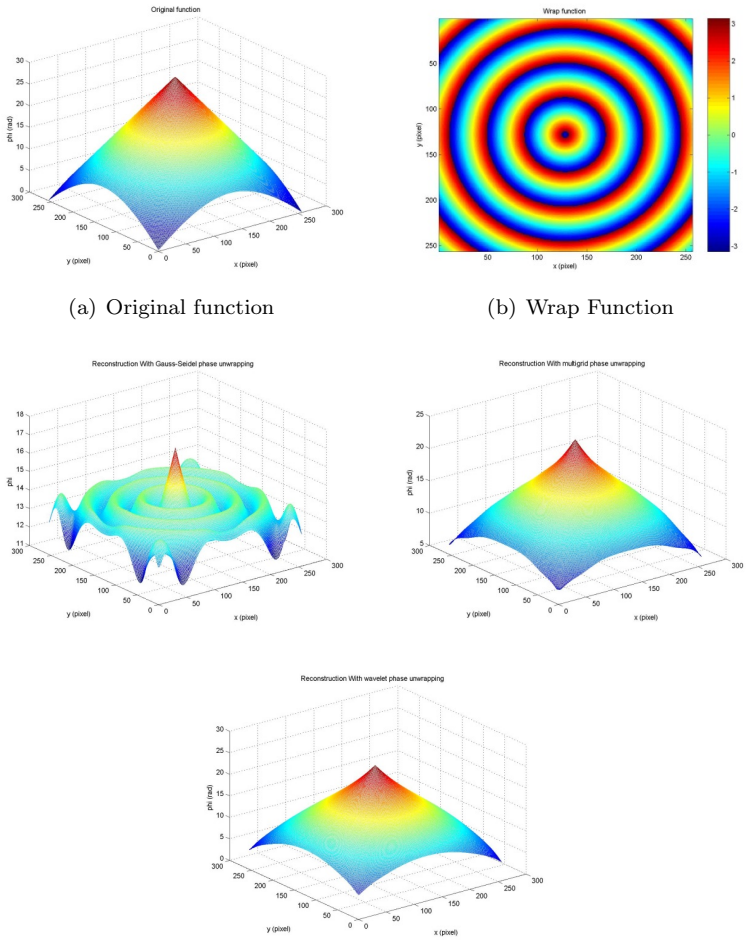

(a) Original function (b) Wrap Function

FIGURE 2. 2(a) Simulated phase pattern, 2(b) wrapped phase, 2(c) unwrapped phase with Gauss-Seidel method, 2(d) unwrapped phase with multigrid, 2(e) unwrapped phase with wavelet.

x and y directions, the same weight function is applied. After the phase unwrapping step by weighted wavelet algorithm, the post-processing step is also performed to achieve congruence between the unwrapped phase and the wrapped phase. In order to construct the DEM, the unwrapped phases were converted to height and then geocoded. To evaluate the results, the DEM generated as the result of InSAR processing was compared with a DEM generated from a 1/25000 scale map. The evaluation was performed in two regions of the Kerman province, Fahraj and Nosratabad, due to reference DEM availability in these two regions. The average amount of height difference between the DEM produced by SAR Interferometry and the reference DEM was 3.05 and 2.60 meter for Fahraj and Nosratabbad, respectively. Our results are in good agreement with the reported accuracy for InSAR

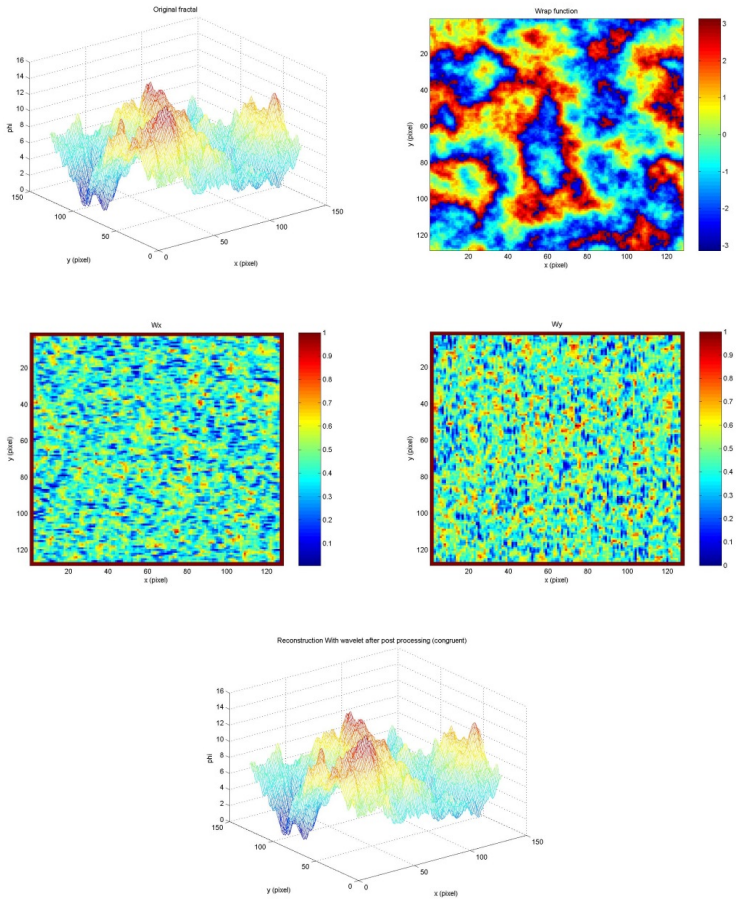

FIGURE 3. 3(a) Simulated phase pattern with fractal, 3(b) wrapped phase, 3(c) weights in x direction, 3(d) weights in y direction, 3(e) unwrapped phase with weighted wavelet phase unwrapping.

method which is between 3 to 20 meters. The reason for better accuracy in Nosrataabad is due to higher coherency in that region.

3.4. **SAR differential interferometry.** To detect the land deformation caused by earthquake, volcano or landslide, it is necessary to compare two images of the same area which are taken exactly from the same position in two different times. In practice, however it is highly improbable that the sensor will return exactly to the same position twice and the baseline will always be different from zero. This causes the presence of a topographic component in the measured interferometric phase, which adds up to the deformation information. The topographic contribution can be separated and subtracted from the deformation by using the so-called differential technique. A second interferogram is generated with two images taken over a time interval during which no significant deformation had occurred. This interferogram,

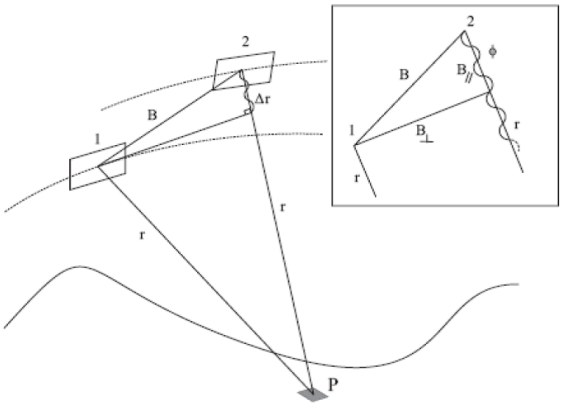

FIGURE 4. SAR interferometry for DEM generation.

which will thus contain only topographic information, is re-scaled and subtracted from the one of interest, leaving in this latter only the deformation signal.

In this experiment three single look complex SAR images of ENVISAT ASAR data were used. Two images were taken before earthquake and one image after earthquake. Figure 5 shows the differential interferogram.

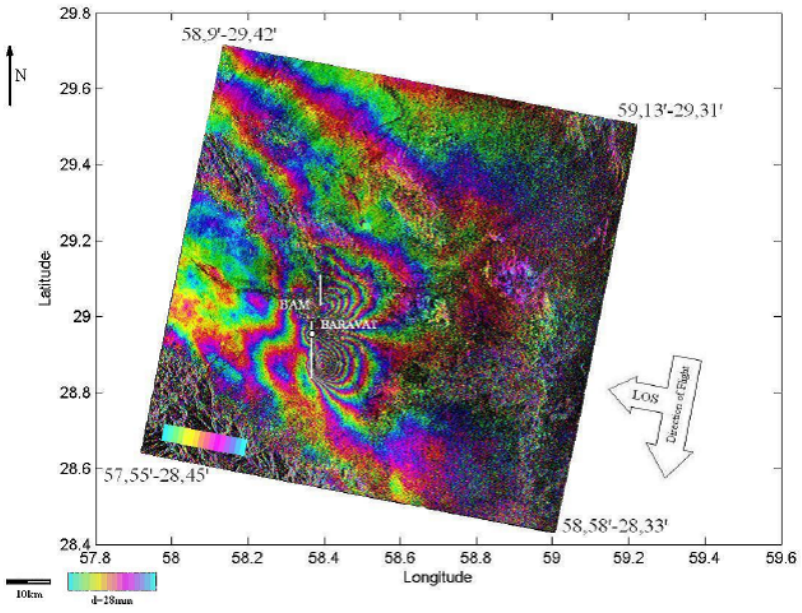

FIGURE 5. Differential interferogram obtained from three SAR images.

The magnitude of the earthquake calculated using the differential SAR interferometry was 6.4 which is in very good agreement with ground-based measurements showing the magnitude of 6.5.

Conclusion. An effective method to solve the phase unwrapping partial differential equation based on the wavelet approach has been discussed. The Wavelet approach overcomes the low convergence rate of Gauss-Seidel relaxation method by transforming low-frequency components of error into high frequency components. By decomposing an image into one low-frequency component (approximation) and three high-frequency components (details) and solving the low-frequency portion of the new system, it speeds up the overall system convergence rate. The proposed algorithm was tested on both simulated and real data; and they shows better result than Gauss-Seidel relaxation and the multigrid methods. Since the new transformed system is mathematically equivalent to the original matrix both for the weighted and unweighted least squares phase unwrapping, its solution is exact to the original equation.

References

[1] T. J. Flynn; *Two-dimensional phase unwrapping with minimum weighted discontinuity*, JOSA A, 14 (1997), pp. 2692–2701.

[2] D. L. Fried; *Least-square fitting a wave-front distortion estimate to an array of phase-difference measurements*, JOSA, 67 (1977), pp. 370–375.

[3] D. C. Ghiglia, L. A. Romero; *Direct phase estimation from phase differences using fast elliptic partial differential equation solvers*, Optics letters, 14 (1989), pp. 1107–1109.

[4] D. C. Ghiglia, L. A. Romero; *Robust two-dimensional weighted and unweighted phase unwrapping that uses fast transforms and iterative methods*, JOSA A, 11 (1994), pp. 107–117.

[5] R. M. Goldstein, H. A. Zebker, C. L. Werner; *Satellite radar interferometry: Two-dimensional phase unwrapping*, Radio Science, 23 (1988), pp. 713–720.

[6] I. Gurov and M. Volkov; *Fringe evaluation and phase unwrapping of complicated fringe patterns by the data-dependent fringe processing method*, Instrumentation and Measurement, IEEE Transactions on, 55 (2006), pp. 1634–1640.

[7] R. H. Hudgin; *Wave-front reconstruction for compensated imaging*, JOSA, 67 (1977), pp. 375–378.

[8] S. B. Kim, Y. S. Kim; *Least squares phase unwrapping in wavelet domain*, IEE Proceedings-Vision, Image and Signal Processing, 152 (2005), pp. 261–267.

[9] Y. Meyer; *Wavelets and operators*, vol. 1, Cambridge university press, 1995.

[10] M. D. Pritt; *Phase unwrapping by means of multigrid techniques for interferometric sar*, Geoscience and Remote Sensing, IEEE Transactions on, 34 (1996), pp. 728–738.

[11] M. D. Pritt, J. S. Shipman; *Least-squares two-dimensional phase unwrapping using fft's*, Geoscience and Remote Sensing, IEEE Transactions on, 32 (1994), pp. 706–708.

[12] M. Rahnemoonfar, B. Plale; *Dem generation with sar interferometry based on weighted wavelet phase unwrapping*, in Computing for Geospatial Research and Application (COM. Geo), 2013 Fourth International Conference on, IEEE, 2013, pp. 87–91.

Maryam Rahnemoonfar

Department of Computer Science, Texas A&M University-Corpus Christi, 6300 Ocean Dr., Corpus Christi, TX 78412, USA

E-mail address: maryam.rahnemoonfar@tamucc.edu